element associated with the nitrogen. As a result, the total $\pi$-electron populations for the "top" and "bottom" halves of pyridine were equal.

The analyses presented herein also led to estimates of the enthalpies of formation of *s*-tetrazine and hexazine. The energies of dissociation to three two-heavy-atom fragments were calculated and were found to become increasingly less endothermic with increasing nitrogen substitution.

In their analysis, Shaik and Hiberty, et al.[7] concluded that "electron delocalization is seldom going to be a driving force in conjugated systems composed of the second row elements C, N and O. These compounds are just about the majority of delocalized species in organic chemistry." It appears to us that electron delocalization is the driving force for the exothermic loss of hydrogen from 1,4-cyclohexadiene to form benzene (in contrast to the strongly endothermic loss of hydrogen from cyclohexene) and for the facile formation of benzene from compounds such as norbornadienone.[46] Many examples of this type could be cited. However, it is also true that some phenomena, which have been explained as resulting from $\pi$-electron delocalization, such as the acidity of carboxylic acids,[47] now appear to have other origins.

(46) Birney, D. M.; Berson, J. A. *J. Am. Chem. Soc.* **1985**, *107*, 4553.
(47) Siggel, M. R.; Thomas, T. D. *J. Am. Chem. Soc.* **1986**, *198*, 4360. Wiberg, K. B.; Laidig, K. E. *Ibid.* **1988**, *10*, 1872. Siggel, M. R.; Streitwieser, A., Jr.; Thomas, T. D. *J. Am. Chem. Soc.* **1988**, *110*, 8022.

**Calculations.** All MO calculations were carried out using GAUSSIAN-82.[48] In most cases, preliminary calculations were carried out using the 3-21G basis set, and for the reduced azines the conformational questions were resolved at this level. The lower energy conformations were then optimized at the 6-31G* level. The geometries of the reduced azines are available as supplementary material. The charge density integrations made use of the PROAIMS package.[49]

**Acknowledgment.** Most of the calculations were carried out using the Pittsburgh Supercomputing Center facilities with the aid of a Cray Research Inc. University Research and Development Grant. This investigation was supported by a grant from the donors of the Petroleum Research Fund, administered by the American Chemical Society.

**Supplementary Material Available:** Tables of the geometries of reduced azines (8 pages). Ordering information is given on any current masthead page.

(48) Binkley, J. S.; Frisch, M. J.; DeFrees, D. J.; Raghavachari, K.; Whiteside, R. A.; Schlegel, H. B.; Fluder, E. M.; Pople, J. A. GAUSSIAN-82, Department of Chemistry, Carnegie-Mellon University, Pittsburgh, PA.
(49) Biegler-Konig, F. W.; Bader, R. F. W.; Tang, T.-H. *J. Comput. Chem.* **1982**, *3*, 317.

# A Priori p$K_a$ Calculations and the Hydration of Organic Anions

**William L. Jorgensen* and James M. Briggs**

*Contribution from the Department of Chemistry, Purdue University, West Lafayette, Indiana 47907.* *Received September 22, 1988*

**Abstract:** A novel theoretical procedure is used to obtain a priori estimates of p$K_a$'s for organic compounds in water. The approach features ab initio molecular orbital calculations for the requisite gas-phase acidities and for development of anion–water intermolecular potential functions. Monte Carlo simulations using statistical perturbation theory are then executed to compute differences in free energies of hydration for the anions and for their conjugate acids. Combination in a thermodynamic cycle yields predicted relative p$K_a$'s for the organic acids in water. The procedure is illustrated for methanethiol, methanol, acetonitrile, methylamine, and ethane. The computed p$K_a$'s for acetonitrile (28) and methylamine (33) are consistent with the rough experimental estimates, while the result of 52 ± 2 for ethane falls in the middle of the broad experimental range for this elusive quantity. The hydration of the anions has also been characterized. In each case, there are four to six particularly strong hydrogen bonds between the anions and water molecules in the first solvation layer.

Investigations of the acidity of organic compounds have played a central role in the development of physical organic chemistry and the conceptual understanding of organic reactivity.[1-5] Knowledge of relative acidities is also critical to the daily activities of synthetic and bioorganic chemists as they formulate viable reaction schemes and mechanisms. Although much organic chemistry is carried out in nonaqueous media, it is notable that the acidity of organic compounds is still usually discussed in terms of p$K_a$'s in water.[1-7] However, this is problematic since the acidity of water itself restricts direct equilibrium measurements to acids with p$K_a$'s below ca. 17. Thus, the experimental p$K_a$'s for weaker acids are typically extrapolated from nonaqueous solvents, come from kinetic measurements, and may be complicated by ion-pairing and aggregation effects.[1,3,5,7-11] The resultant uncertainties can be substantial, as reflected in the reported range of aqueous p$K_a$'s for the extreme case of methane and ethane which covers from 40 to 60.[1,7,10,11]

(1) Cram, D. J. *Fundamentals of Carbanion Chemistry*; Academic Press: New York, 1965.
(2) Bordwell, F. G. *Acc. Chem. Res.* **1988**, *21*, 456. Taft, R. W.; Bordwell, F. G. *Acc. Chem. Res.* **1988**, *21*, 463.
(3) Streitwieser, A., Jr.; Juaristi, E.; Nebenzahl, L. L. In *Comprehensive Carbanion Chemistry*; Buncel, E., Durst, T., Eds.; Elsevier: Amsterdam, 1980; Part A, Chapter 7.
(4) Taft, R. W. *Prog. Phys. Org. Chem.* **1983**, *14*, 247.
(5) Lowry, T. H.; Richardson, K. S. *Mechanism and Theory in Organic Chemistry*, 3rd ed.; Harper & Row: New York, 1987; Chapter 3.
(6) Arnett, E. M.; Scorrano, G. *Adv. Phys. Org. Chem.* **1976**, *13*, 85.
(7) Stewart, R. *The Proton: Applications to Organic Chemistry*; Academic Press: New York, 1985.
(8) Pearson, R. G.; Dillon, R. L. *J. Am. Chem. Soc.* **1953**, *75*, 2439.
(9) Streitwieser, A., Jr. *Acc. Chem. Res.* **1984**, *17*, 353.
(10) Juan, B.; Schwarz, J.; Breslow, R. *J. Am. Chem. Soc.* **1980**, *102*, 5741.
(11) Butin, K. P.; Beletskaya, I. P.; Kashin, A. N.; Reutov, O. A. *J. Organomet. Chem.* **1967**, *10*, 197.

0002-7863/89/1511-4190$01.50/0 

Under the circumstances, it is clearly desirable to have general theoretical approaches to the accurate computation of $pK_a$'s for organic compounds in water. As described in brief previously,[12] such a procedure has been developed with use of both high-level quantum and statistical mechanical methods. Consideration of the thermodynamic cycle

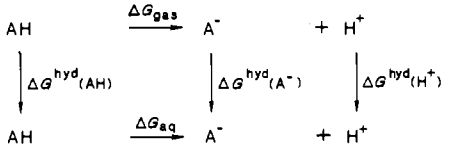


yields eq 1 in which the aqueous $pK_a$ for the acid AH is given by

$$\Delta G_{aq} = 2.3RT\ pK_a(AH) = \Delta G_{gas} + \Delta G^{hyd}(A^-) + \Delta G^{hyd}(H^+) - \Delta G^{hyd}(AH) \quad (1)$$

the gas-phase acidity and the difference in free energies of hydration for the acid and the two ions. The gas-phase acidity can be routinely computed by ab initio molecular orbital methods with good accuracy for molecules with up to at least six non-hydrogen atoms.[12-15] Furthermore, free energies of hydration from the gas phase can be computed from Monte Carlo statistical mechanics or molecular dynamics simulations in which the ion or molecule is effectively made to disappear in water.[16,17] However, improved precision and accuracy can be obtained by calculating differences in free energies of hydration as one molecule or ion is mutated into another during the simulations.[18] This suggests computing the difference in $pK_a$'s for two acids, AH and BH. Subtraction of the corresponding pair of expressions analogous to eq 1 then yields eq 2. Specifically, the difference in $pK_a$'s is given by the

$$2.3RT\ [pK_a(BH) - pK_a(AH)] = \Delta\Delta G_{gas}(BH - AH) + \Delta\Delta G^{hyd}(B^- - A^-) - \Delta\Delta G^{hyd}(BH - AH) \quad (2)$$

difference in gas-phase acidities plus the difference in free energies of hydration for the anions and acids. The last two terms in eq 2 require the performance of simulations in which $A^-$ and AH are gradually converted into $B^-$ and BH, and the differences in free energies are accumulated. The first calculations of this type for organic solutes in water were reported in 1985 and used statistical perturbation theory to obtain the free energy changes with excellent precision.[18] This was the technical development that was required to facilitate the present approach to computing relative $pK_a$'s. It may be noted that the approach avoids the necessity of computing $\Delta G^{hyd}$ for a proton and the combination of numbers with large magnitudes implicit in eq 1. Also, from an experimental standpoint, the generally unavailable term on the right-hand side of eq 2 is the difference in free energies of hydration for the anions; the other two terms can be obtained from gas-phase measurements and solubility data.

In the initial report, the $pK_a$'s of acetonitrile and ethane were computed relative to methanethiol.[12] As presented here, another series consisting of methanol, methylamine, and ethane has now also been considered. This provides a second, independent estimate for the $pK_a$ of ethane as well as a value for the parent alkylamine. In addition, details on the development of the anion–water potential functions, which are the critical component in the fluid simulations, are presented along with quantitative and qualitative results on the hydration of the five anions.

There has been little related, earlier theoretical work, though a paper by Warshel et al. should be noted.[19] They carried out molecular dynamics simulations to compute the difference in free energies of hydration for the conversions of two acid groups to the carboxylates in bovine pancreatic trypsin inhibitor, i.e., combination of the second and fourth terms on the right-hand side of eq 1. Very recently, Guissani et al. reported a calculation of the pH of water essentially via computing the terms in eq 1.[20] Particle insertion methods were used to obtain the free energies of hydration of $H_2O$, $H_3O^+$, and $OH^-$. The magnitudes of the individual terms in eq 1 and the application of particle insertion methods to such dense fluids make this approach difficult. Less closely related studies have used simulation methods and other thermodynamic cycles to compute relative free energies of binding for host–guest complexes[21-25] and redox potential differences for quinones.[26]

## Computational Procedure

**Quantum Mechanics.** Ab initio molecular orbital calculations were used to calculate the gas-phase acidities ($\Delta G_{gas}$) for the five acids, methanethiol, methanol, acetonitrile, methylamine, and ethane, and to develop the corresponding anion–water potential functions for the fluid simulations. All calculations employed the 6-31+G(d) basis set which includes a set of d-type polarization functions and a set of diffuse s and p orbitals on all non-hydrogen atoms.[27] The diffuse functions are well-known to be important in properly describing the electronic structure of anions and in obtaining accurate results for $\Delta G_{gas}$.[13-15,28]

In order to compute the gas-phase acidities, full geometry optimizations were performed for the acids and anions with the 6-31+G(d) basis set. The correlation energies were then computed with Møller–Plesset theory to third order.[28] Thus, the standard notation for the calculations is MP3/MP2/6-31+G(d)//6-31+G(d).[28] The MP3/MP2 calculations did not include the core orbitals and are generally comparable to configuration interaction with full double excitations. The zero-point vibrational energies for the acids and anions were then computed from frequency calculations at the 6-31+G(d) level. The frequencies and geometrical results also allowed computation of the entropy change at 298 K for the ionization ($AH \rightarrow A^- + H^+$) according to standard formulas.[28] The enthalpy changes were obtained from eq 3, where $\Delta E_e°$ is

$$\Delta H^{298} = \Delta E_e° + \Delta E_v° + \Delta(\Delta E_v^{298}) + \Delta E_r^{298} + \Delta E_t^{298} + \Delta(PV) \quad (3)$$

the electronic energy change including the correlation energies, $\Delta E_v°$ is the change in the zero-point energy, $\Delta(\Delta E_v^{298})$ is the change in the vibrational energy on going to 298 K, and the remaining quantities are for the changes in rotational and translational energy and the work term which were treated classically. Vibrations with frequencies below 500 $cm^{-1}$ were treated as classical rotations in computing $\Delta E_v°$ and $\Delta(\Delta E_v^{298})$. Finally, the enthalpy and entropy changes were combined to give $\Delta G_{gas}$. It should be noted that ethyl anion is probably not bound in the gas phase with respect to loss of an electron.[29-31] Since the present calculations utilized restricted Hartree–Fock theory, this issue was not reinvestigated and the model with paired electrons is reasonable if the anion is bound in water.

The development of the anion–water potential functions entailed 6-31+G(d) calculations for different orientations of a water molecule about the anions. For each ion, four or five low-energy orientations were considered and one or two key intermolecular geometrical variables were optimized; the geometries of the anions were fixed in their 6-31+G(d) optimized forms and the experimental geometry was adopted for water

(12) Jorgensen, W. L.; Briggs, J. M.; Gao, J. *J. Am. Chem. Soc.* **1987**, *109*, 6857.
(13) Chandrasekhar, J.; Andrade, J. G.; Schleyer, P. v. R. *J. Am. Chem. Soc.* **1981**, *103*, 5609.
(14) Gao, J.; Garner, D. S.; Jorgensen, W. L. *J. Am. Chem. Soc.* **1986**, *108*, 4784.
(15) Siggel, M. R. F.; Thomas, D. T.; Saethre, L. J. *J. Am. Chem. Soc.* **1988**, *110*, 91.
(16) Jorgensen, W. L.; Blake, J. F.; Buckner, J. K. *Chem. Phys.* **1989**, *129*, 193.
(17) Cieplak, P.; Kollman, P. A. *J. Am. Chem. Soc.* **1988**, *110*, 3734.
(18) Jorgensen, W. L.; Ravimohan, C. *J. Chem. Phys.* **1985**, *83*, 3050.
(19) Warshel, A.; Sussman, F.; King, G. *Biochemistry* **1986**, *25*, 8368.
(20) Guissani, Y.; Guillot, B.; Bratos, S. *J. Chem. Phys.* **1988**, *88*, 5850.
(21) Lybrand, T. P.; McCammon, J. A.; Wipff, G. *Proc. Natl. Acad. Sci. U.S.A.* **1986**, *83*, 833.
(22) Wong, C. F.; McCammon, J. A. *J. Am. Chem. Soc.* **1986**, *108*, 3830.
(23) Bash, P. A.; Singh, U. C.; Brown, F. K.; Langridge, R.; Kollman, P. A. *Science* **1987**, *235*, 574.
(24) Rao, S. N.; Singh, U. C.; Bash, P. A.; Kollman, P. A. *Nature* **1987**, *328*, 551.
(25) Jorgensen, W. L.; Boudan, S.; Nguyen, T. B. *J. Am. Chem. Soc.* **1989**, *111*, 755.
(26) Reynolds, C. A.; King, P. M.; Richards, W. G. *Nature* **1988**, *334*, 80.
(27) Clark, T.; Chandrasekhar, J.; Spitznagel, G. W.; Schleyer, P. v. R. *J. Comput. Chem.* **1983**, *4*, 294. Frisch, M. J.; Pople, J. A.; Binkley, J. S. *J. Chem. Phys.* **1984**, *80*, 3265, footnote 13.
(28) Hehre, W. J.; Radom, L.; Schleyer, P. v. R.; Pople, J. A. *Ab Initio Molecular Orbital Theory*; Wiley: New York, 1986.
(29) DePuy, C. H.; Bierbaum, V. M.; Damrauer, R. *J. Am. Chem. Soc.* **1984**, *106*, 4051.
(30) Schleyer, P. v. R.; Spitznagel, G. W.; Chandrasekhar, J. *Tetrahedron Lett.* **1986**, *27*, 4411.
(31) Graul, S. T.; Squires, R. R. *J. Am. Chem. Soc.* **1988**, *110*, 607.

as in the TIP4P model,[32] which was used in the simulations. The resultant interaction energies and geometrical data then provided a basis for determining the requisite parameters for the intermolecular potential functions, as discussed below. It has been found previously that 6-31+G(d) calculations give excellent results for anion–water interaction energies in comparison with experimental data.[14] The differences in the computed $\Delta E$s and experimental $\Delta H$s are typically less than 1 kcal/mol. Furthermore, new experimental data fully support the predictive abilities of the calculations.[33]

All of the ab initio calculations were executed with the GAUSSIAN/82 program[34] on a Gould 32/8750 computer in our laboratory.

**Statistical Mechanics.** The differences in free energies of hydration were obtained from Monte Carlo simulations with the same procedures as described previously for the interconversion of methanol and ethane in water.[18] Briefly, the systems consisted of the solute plus 216 TIP4P water molecules in a cubic box with periodic boundary conditions. The simulations were performed in the NPT ensemble at 25 °C and 1 atm. Metropolis sampling was augmented by preferential sampling in which the probability of attempting to move a solvent molecule was made proportional to $1/(r^2 + 120\ \text{Å}^2)$ where $r$ is a solute–water oxygen distance.[35] An attempt to move the solute was made on every 50th configuration, and a change in the volume was tried on every 1250th configuration. The ranges for the moves were adjusted to provide a ca. 40% acceptance probability for new configurations. The intermolecular interactions were quadratically feathered to zero between 8.0 and 8.5 Å based roughly on the center-of-mass separations.

The free energy changes, $\Delta\Delta G^{hyd}$, were obtained by applying statistical perturbation theory[36] and mutating one neutral solute to another or one anion to another in a series of simulations.[18] The computations are based on eq 4, which states that the difference in free energies between the

$$G_P - G_R = -k_B T \ln \langle \exp(-(H_P - H_R)/k_B T) \rangle_R \quad (4)$$

reference (R) and perturbed (P) systems is a function of their energy difference that can be obtained by averaging during a simulation for R. For the present solutes, the differences are too large to span in one perturbation step. Consequently, three simulations were used to interconvert the acids and four were used for the anions. A coupling parameter $\lambda$ was designated to reflect the gradual mutation of solute A to B according to eq 5 where $\lambda$ goes from 0 to 1 and $\zeta$ represents the potential

$$\zeta_\lambda = \zeta_A + \lambda(\zeta_B - \zeta_A) \quad (5)$$

function and geometrical parameters. Double-wide sampling was performed, so for a simulation at $\lambda$, perturbations were made to both $\lambda + \Delta\lambda$ and $\lambda - \Delta\lambda$.[18] Thus, for the acids and anions the average values of $\Delta\lambda$ were 0.167 and 0.125, respectively.

Each simulation had an equilibration phase of ca. $10^6$ configurations followed by averaging over an additional $1.5 \times 10^6$ or $2.0 \times 10^6$ configurations. In the calculations, the initial and final solutes were overlaid in a logical way. For example, in mutating $CH_3O^-$ to $CH_3NH^-$, the O and N were kept coincident, as were the CO and CN axes. Basically, the methyl group had to be pushed out a little along the axis and the hydrogen grown out on N. This hydrogen started ($\lambda = 0$) as a dummy atom on O with a bond length of 0.5 Å and ended up ($\lambda = 1$) as the real atom on N with a bond length of 1.014 Å.

Following these calculations, an additional Monte Carlo simulation was carried out for each anion in water to obtain the structural results reported below. This was necessary because the perturbation calculations were only run for $\lambda$ values between 0 and 1. For these supplemental calculations, the equilibration period was $5 \times 10^5$ configurations with averaging over an additional $1 \times 10^6$ configurations.

The statistical mechanics simulations were all performed with the BOSS program on the Gould 32/8750 computer.

**Potential Functions.** The water–water and solute–water interactions were described by potential functions in the standard Lennard-Jones plus Coulomb format (eq 6).[37] The ions and molecules are represented by

$$\Delta E_{ab} = \sum_i^{\text{on a}} \sum_j^{\text{on b}} (q_i q_j e^2/r_{ij} + A_{ij}/r_{ij}^{12} - C_{ij}/r_{ij}^6) \quad (6)$$

Table I. Potential Function Parameters for the Neutral Molecules

| site | $q$, e$^{-1}$ | $\sigma$, Å | $\epsilon$, kcal/mol |
|---|---|---|---|
| | $CH_3SH$ | | |
| $CH_3$ | 0.180 | 3.775 | 0.207 |
| S | −0.450 | 3.550 | 0.250 |
| H | 0.270 | 0.0 | 0.0 |
| | $CH_3OH$ | | |
| $CH_3$ | 0.265 | 3.775 | 0.207 |
| O | −0.700 | 3.070 | 0.170 |
| H | 0.435 | 0.0 | 0.0 |
| | $CH_3CN$ | | |
| $CH_3$ | 0.150 | 3.775 | 0.207 |
| C | 0.280 | 3.650 | 0.150 |
| N | −0.430 | 3.200 | 0.170 |
| | $CH_3NH_2$ | | |
| $CH_3$ | 0.200 | 3.775 | 0.207 |
| N | −0.900 | 3.250 | 0.170 |
| H | 0.350 | 0.0 | 0.0 |
| | $CH_3CH_3$ | | |
| $CH_3$ | 0.0 | 3.775 | 0.207 |

Table II. Potential Function Parameters for the Anions

| site | $q$, e$^-$ | $\sigma$, Å | $\epsilon$, kcal/mol |
|---|---|---|---|
| | $CH_3S^-$ | | |
| C | −0.40 | 4.20 | 0.30 |
| H | 0.10 | 2.50 | 0.05 |
| S | −0.90 | 4.25 | 0.50 |
| | $CH_3O^-$ | | |
| C | −0.20 | 4.20 | 0.30 |
| H | 0.06 | 2.50 | 0.05 |
| O | −0.98 | 3.15 | 0.25 |
| | $CH_2CN^-$ | | |
| C1 | −1.07 | 4.20 | 0.30 |
| H | 0.19 | 2.50 | 0.05 |
| C2 | 0.51 | 3.65 | 0.15 |
| N | −0.82 | 3.40 | 0.25 |
| | $CH_3NH^-$ | | |
| C | −0.30 | 4.20 | 0.30 |
| H | 0.07 | 2.50 | 0.05 |
| N | −1.31 | 3.40 | 0.25 |
| H | 0.40 | 2.50 | 0.05 |
| | $CH_3CH_2^-$ | | |
| $C_2$ | −0.40 | 4.20 | 0.30 |
| H2 | 0.08 | 2.50 | 0.05 |
| C1 | 0.00 | 4.20 | 0.30 |
| H1 | 0.07 | 2.50 | 0.05 |
| M[a] | −0.98 | 0.0 | 0.0 |

[a] M is in a lone-pair position with $r$(C1M) = 0.35 Å and ∠C2C1M = 117.75°.

interaction sites located usually on nuclei that have associated charges, $q_i$, and Lennard-Jones parameters, $\sigma_i$ and $\epsilon_i$. The latter are related to $A_{ij}$ and $C_{ij}$ by $A_{ii} = 4\epsilon_i\sigma_i^{12}$, $C_{ii} = 4\epsilon_i\sigma_i^6$, $A_{ij} = (A_{ii}A_{jj})^{1/2}$, and $C_{ij} = (C_{ii}C_{jj})^{1/2}$.

The OPLS parameters and experimental geometries were used for $CH_3SH$,[38] $CH_3OH$,[38] $CH_3CN$,[39] and $CH_3CH_3$[40] along with the compatible TIP4P model for water.[32] These potential functions have been derived by fitting to experimental data to give excellent descriptions of the structures and thermodynamic properties of the pure liquids.[32,37-40] As summarized in Table I, parameters have also been derived for methylamine in the same manner for the present study. They yield errors of 1% for the density and heat of vaporization of liquid methylamine at its boiling point, −6.3 °C at 1 atm.[41]

The parameters derived here for the anions are summarized in Table II. All atoms are explicit in these cases, whereas a united-atom representation is used for the methyl groups of the neutral molecules (Table

(32) Jorgensen, W. L.; Chandrasekhar, J.; Madura, J. D.; Impey, R. W.; Klein, M. L. *J. Chem. Phys.* **1983**, *79*, 926. Jorgensen, W. L.; Madura, J. D. *Mol. Phys.* **1985**, *56*, 1381.

(33) Meot-Ner, M.; Sieck, L. W. *J. Phys. Chem.* **1986**, *90*, 6687. Meot-Ner, M., submitted for publication.

(34) Binkley, J. S.; Whiteside, R. A.; Raghavachari, K.; Seeger, R.; DeFrees, D. J.; Schlegel, H. B.; Frisch, M. J.; Pople, J. A.; Kahn, L. R. *GAUSSIAN 82 Release H*; Carnegie-Mellon University: Pittsburgh, PA, 1982. Converted to the Gould 32/8750 by Dr. J. D. Madura and J. F. Blake.

(35) Owicki, J. C. *ACS Symp. Ser.* **1978**, *No. 86*, 159.

(36) Zwanzig, R. W. *J. Chem. Phys.* **1954**, *22*, 1420.

(37) Jorgensen, W. L.; Tirado-Rives, J. *J. Am. Chem. Soc.* **1988**, *110*, 1657.

(38) Jorgensen, W. L. *J. Phys. Chem.* **1986**, *90*, 1276, 6379.

(39) Jorgensen, W. L.; Briggs, J. M. *Mol. Phys.* **1988**, *63*, 547.

(40) Jorgensen, W. L.; Madura, J. D.; Swenson, C. J. *J. Am. Chem. Soc.* **1984**, *106*, 6638.

(41) Briggs, J. M.; Jorgensen, W. L., unpublished results.

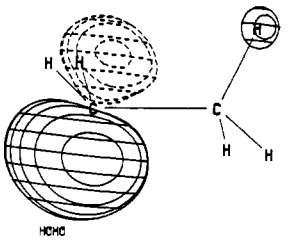


**Figure 1.** Highest occupied molecular orbital of the ethyl anion as depicted by the PSI/77 program from an ab initio 3-21G wave function.[43] The contour level is ± 0.1 au.

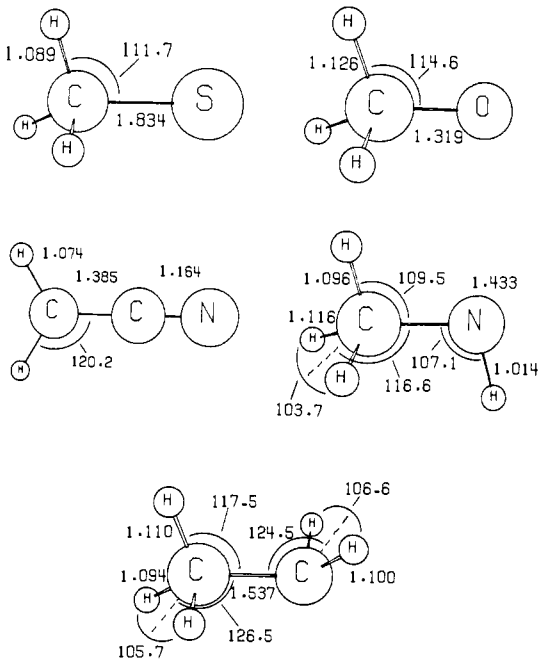


**Figure 2.** Geometries optimized for the five anions with the 6-31+G(d) basis set.

I). The additional hydrogens were needed to provide viable charge distributions for reproducing the ab initio results. No lone-pair-type interaction sites were required to fit the ab initio data except in the case of ethyl anion. This reflects the shape of its highest occupied molecular orbital, which is illustrated in Figure 1. The other anions each have two or three high-lying lone-pair orbitals that allow the electric field to be represented acceptably by sites centered on the highly charged atoms. The 6-31+G(d) geometries were used for the anions in the simulations and were kept fixed. In the prior ab initio study,[14] it was found that complexation with one water molecule has insignificant effect on the geometries of such anions, e.g., bond lengths vary by less than 0.01 Å. Furthermore, there is computational evidence that additional hydration should have negligible impact as well.[42] The distortions of the water molecules in the complexes are also slight, e.g., $\Delta r$(OH) is less than 0.04 Å.[14]

It should be noted in Tables I and II that the number of unique sets of Lennard-Jones parameters is minimal, e.g., all hydrogens, the methyl carbons, and the nitrogens in the anions have the same $\sigma$'s and $\epsilon$'s. Thus, the parameter fitting for the anions focused on the charge distributions. Overall, there was limited latitude in the parameter selection since the $\sigma$'s were required to be consistent with prior values for the atom types, the $\epsilon$'s were set to standard values since the attractive energetics are overwhelmingly dominated by the electrostatic interactions, and the charges must be qualitatively reasonable and consistent with prior values.[37-40]

## Results and Discussion

**Gas-Phase Acidities.** The optimized geometries for the anions are displayed in Figure 2. The total energies and results for the neutral molecules are provided in the supplementary material in

(42) Morokuma, K. *J. Am. Chem. Soc.* **1982**, *104*, 3732. Jorgensen, W. L.; Buckner, J. K. *J. Phys. Chem.* **1986**, *90*, 4651.
(43) Jorgensen, W. L. *QCPE* **1980**, *12*, *No. 340*.

**Table III.** Calculated Gas-Phase Enthalpy Components (kcal/mol) for AH → A$^-$ + H$^+$

| AH | $\Delta E_e°$ | $\Delta E_v°$ | $\Delta(\Delta E_v)^{298}$ | $\Delta E_r^{298}$ | $\Delta E_t^{298}$ | $\Delta(PV)$ |
|---|---|---|---|---|---|---|
| $CH_3SH$ | 361.1 | −6.4 | −0.01 | −0.30 | 0.89 | 0.59 |
| $CH_3OH$ | 390.3 | −9.9 | −0.02 | −0.30 | 0.89 | 0.59 |
| $CH_3CN$ | 384.9 | −10.4 | 0.19 | 0.0 | 0.89 | 0.59 |
| $CH_3NH_2$ | 415.4 | −11.5 | −0.08 | 0.0 | 0.89 | 0.59 |
| $CH_3CH_3$ | 432.9 | −11.2 | 0.01 | 0.0 | 0.89 | 0.59 |

**Table IV.** Gas-Phase Free Energy, Enthalpy, and Entropy Changes at 25 °C for AH → A$^-$ + H$^+$

| | calcd[a] | | | exptl[a,b] | | |
|---|---|---|---|---|---|---|
| AH | $\Delta G$ | $\Delta H$ | $\Delta S$ | $\Delta G$ | $\Delta H$ | $\Delta S$ |
| $CH_3SH$ | 349.5 | 355.9 | 21.6 | 352.7 | 359.0 | 21 |
| $CH_3OH$ | 375.0 | 381.6 | 22.0 | 372.6 | 379.2 | 22 |
| $CH_3CN$ | 367.7 | 376.2 | 28.6 | 364.4 | 372.1 | 26 |
| $CH_3NH_2$ | 397.8 | 405.3 | 25.2 | 395.7 | 403.2 | 25 |
| $CH_3CH_3$ | 414.5 | 423.2 | 29.3 | 413.5 | 421[c] | (25)[d] |

[a] Energies in kcal/mol; entropies in cal/mol-K. [b] Reference 45. [c] Reference 29. [d] Reference 46.

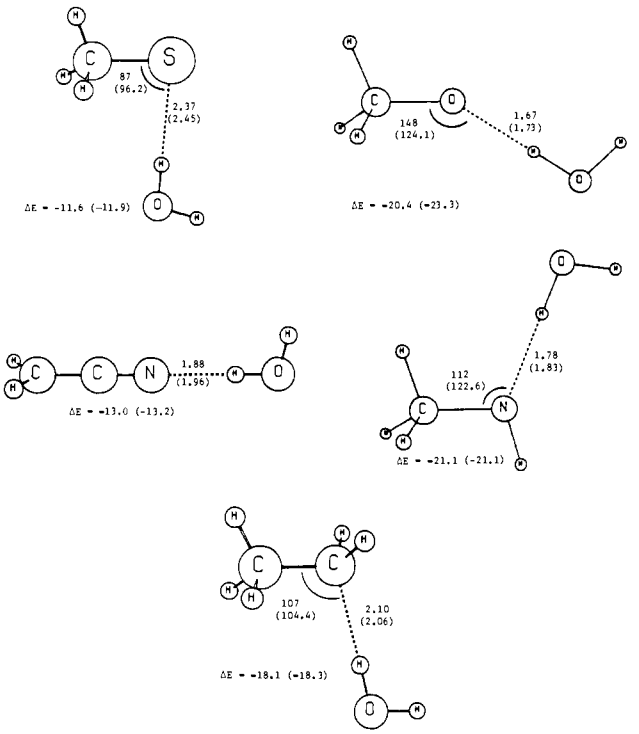


**Figure 3.** Lowest energy forms for the anion–water complexes, partially optimized with 6-31+G(d) calculations. The results from the potential functions for the interaction energies and optimized geometrical variables are shown with the corresponding 6-31+G(d) results in parentheses. Distances are in Å, angles in degrees, and $\Delta E$ in kcal/mol.

Z-matrix format. It may be noted that the ethyl anion is distinctly pyramidal, which leads to the HOMO in Figure 1. Also, in the simulations and in Figure 2, $CH_2CN^-$ has been treated as planar. Actually, the true minimum has a slightly pyramidalized carbon; this form is 0.10 kcal/mol lower in energy than the planar alternative at the 6-31+G(d) level[44] and was used in computing the gas-phase acidity.

The components from eq 3 for the computation of $\Delta H$ are listed in Table III, while Table IV contains the computed and experimental free energies, enthalpies, and entropies. The quality of

(44) Kaneti, J.; Schleyer, P. v. R.; Clark, T.; Kos, A. J.; Spitznagel, G. W.; Andrade, J. G.; Moffat, J. B. *J. Am. Chem. Soc.* **1986**, *108*, 1481.
(45) Bartmess, J. E.; McIver, R. T., Jr. In *Gas Phase Ion Chemistry*; Bowers, M. T., Ed.; Academic Press: New York, 1979; Vol. 2, p 87. Lias, S. G.; Bartmess, J. E.; Liebman, J. F.; Holmes, J. L.; Levin, R. D.; Mallard, W. G. *J. Phys. Chem. Ref. Data* **1988**, *17* (S1), 1–872.

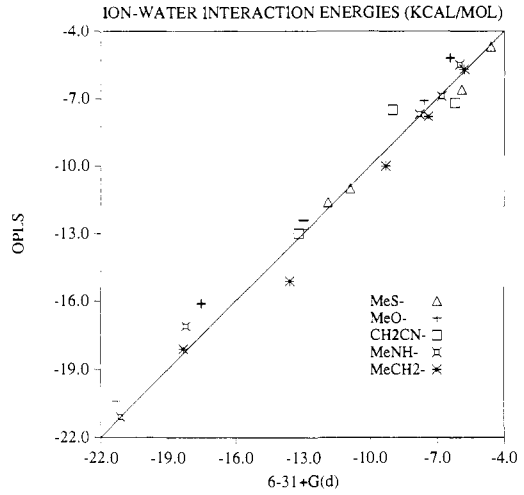


**Figure 4.** Comparison of the interaction energies for the 22 anion–water complexes computed with the 6-31+G(d) calculations and the potential functions.

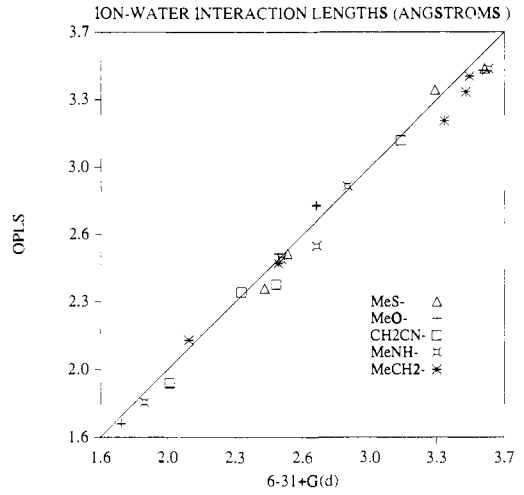


**Figure 5.** Comparison of anion–water distances (Å) for the 22 complexes computed with the 6-31+G(d) calculations and the potential functions.

the present level of ab initio theory is apparent; the average error in the computed free energies is 2.4 kcal/mol. It should be noted that the experimental $\Delta H$ for ethane is ambiguous owing to the instability of the anion.[29] However, the extrapolated experimental result and the computed value for the bound anion are consistent. Also, a standard entropy change of 25 cal/mol-K has been assumed for ethane[46] and is supported by the constancy of the observed and calculated results for $\Delta S$ in Table IV.

**Anion–Water Complexes.** The lowest energy forms for the five anion–water complexes that were examined are illustrated in Figure 3. The optimized geometrical parameters and interaction energies from the potential functions are given along with the 6-31+G(d) predictions in parentheses. In all, the potential function parameters in Table II were obtained by fitting to the 6-31+G(d) results for 22 such complexes with different dispositions of the water molecule. The quality of the fit is illustrated in Figures 4 and 5, which compare the results from the 6-31+G(d) calculations and the potential functions for the interaction energies and optimized anion–water distances for all 22 complexes. The standard deviations for the energies and distances are 0.5 kcal/mol and 0.05 Å. The complete results for the 22 complexes are given in the supplementary material. Low-energy geometries were focused on since they are heavily sampled in the simulations. Overall, the reproduction of the 50 ab initio data points (interaction energies, anion–water distances and angles) for these key geometries is pleasing in view of the effectively small number of independent fitting parameters discussed above and the simplicity of the point charge models.

(46) Pearson, R. G. *J. Am. Chem. Soc.* **1986**, *108*, 6109.

**Table V.** Relative Free Energies of Hydration (kcal/mol) at 25 °C

| | calcd | | |
|---|---|---|---|
| AH → BH | $\Delta\Delta G^{hyd}$ (B⁻ − A⁻) | $\Delta\Delta G^{hyd}$ (BH − AH) | exptl[a] $\Delta\Delta G^{hyd}$ (BH − AH) |
| $CH_3SH \rightarrow CH_3CN$ | 5.2 ± 0.4 | −1.3 ± 0.2 | −2.6 |
| $CH_3SH \rightarrow CH_3CH_3$ | −6.4 ± 0.2 | 3.9 ± 0.1 | 3.1 |
| $CH_3OH \rightarrow CH_3NH_2$ | 2.8 ± 0.2 | 1.3 ± 0.1 | 0.5 |
| $CH_3OH \rightarrow CH_3CH_3$ | 20.4 ± 0.2 | 6.8 ± 0.2 | 6.9 |
| $CH_3OH \rightarrow CH_3SH$ | 27.4 ± 0.3 | 3.1 ± 0.1 | 3.8 |

[a] References 46 and 48.

Returning to Figure 3, the hydrogen-bonded structures for these most bound complexes are all reasonable and consistent with prior results.[14,33] From 6-31+G(d) calculations on fully optimized 6-31G(d) geometries,[14] the global minima for $CH_3S^-$---$H_2O$ and $CH_3O^-$---$H_2O$ have interaction energies of −12.3 and −22.3 kcal/mol as compared to −11.9 and −21.3 kcal/mol from the partially optimized 6-31+G(d) results in Figure 3. Experimental $\Delta H$s are available for two of the complexes;[33] Meot-Ner has obtained −23.9 kcal/mol for $CH_3O^-$---$H_2O$ and −13.2 kcal/mol for $CH_2CN^-$---$H_2O$. The present results are −21.3 and −13.2 from the 6-31+G(d) calculations and −20.4 and −13.0 from the potential functions. Meot-Ner also found −14.2 kcal/mol for $HS^-$---$H_2O$, which varies from our best estimate by 1.2 kcal/mol[14] and is somewhat lower than the −11.9 and −11.6 kcal/mol for $CH_3S^-$---$H_2O$ in Figure 3. The remaining two complexes, $CH_3NH^-$---$H_2O$ and $CH_3CH_2^-$---$H_2O$, are undoubtedly not energy minima in isolation and would undergo proton transfer, if the geometry of water was not constrained.

The present order of hydrogen bond strengths should be noted: $CH_3O^- \simeq CH_3NH^- > CH_3CH_2^- > CH_2CN^- \simeq CH_3S^-$. Since the potential functions (eq 6) employ fixed charges and consequently can only represent polarization effects in an average sense, possible errors from this source can be limited by comparing ions with similar ion–water interaction energies. Thus, the perturbation calculations were carried out for mutating $CH_3O^-$ to $CH_3NH^-$ and $CH_3CH_2^-$, and for converting $CH_3S^-$ to $CH_2CN^-$ and $CH_3CH_2^-$. Without explicit polarization, the tendency is to obtain computed heats of solution that are progressively too exothermic as the individual ion–solvent interactions become stronger.[16,47] Thus, going from $CH_3O^-$ to $CH_3CH_2^-$ should somewhat underestimate the hydration of $CH_3CH_2^-$ and lead to a too positive $pK_a$ for ethane, while the $CH_3S^-$ to $CH_3CH_2^-$ transformation should lead to an underestimate of the $pK_a$ and close the bracket.

**Aqueous Acidities.** The relative free energies of hydration computed in the Monte Carlo simulations are summarized in Table V for both the anions and acids. The experimental results are only shown for the acids, though data for the anions could be obtained by working backwards from the measured $pK_a$'s via eq 2. However, the uncertainties in the experimental $pK_a$'s for $CH_3CN$, $CH_3NH_2$, and $CH_3CH_3$ are too large to make the comparisons worthwhile. The reported statistical uncertainties in the computed results are $\pm 1\sigma$ and were obtained from separate averages over blocks of $1 \times 10^5$ configurations.

For the anions, the more charge-delocalized $CH_2CN^-$ ion is found to be less well hydrated than the thiolate ion by 5.2 kcal/mol, while the stronger ion–water interactions for ethyl anion (Figure 3) make it better hydrated than $CH_3S^-$ by 6.4 kcal/mol. Furthermore, $CH_3NH^-$ is predicted to be less well hydrated than $CH_3O^-$ by 2.8 kcal/mol, and the stronger ion–water interactions and more open anionic site for $CH_3O^-$ make it better hydrated than $CH_3CH_2^-$ by 20.4 kcal/mol. Methoxide ion is also found to be much better hydrated than methanethiolate; however, based

(47) Chandrasekhar, J.; Spellmeyer, D. C.; Jorgensen, W. L. *J. Am. Chem. Soc.* **1984**, *106*, 903.
(48) Ben-Naim, A.; Marcus, Y. *J. Chem. Phys.* **1984**, *81*, 2016. Dec, S. F.; Gill, S. J. *J. Solution Chem.* **1984**, *13*, 27.
(49) Bonhoeffer, K. F.; Gieb, K. H.; Reitz, O. *J. Chem. Phys.* **1939**, *7*, 664.
(50) Fishbein, J. C.; Jencks, W. P. *J. Am. Chem. Soc.* **1988**, *110*, 5087.

**Table VI.** Gas-Phase Free Energy Differences (kcal/mol) and Aqueous $pK_a$'s at 25 °C

| | $\Delta\Delta G_{gas}$(BH − AH) | | $pK_a$(BH) | |
|---|---|---|---|---|
| AH → BH | calcd | exptl[a] | calcd | exptl |
| $CH_3SH \rightarrow CH_3CN$ | 18.2 | 11.7 | 28.4 ± 0.3 | 24–27[b] |
| $CH_3SH \rightarrow CH_3CH_3$ | 65.0 | 61 | 50.4 ± 0.2 | 42–60[c] |
| $CH_3OH \rightarrow CH_3NH_2$ | 22.8 | 23.1 | 33.3 ± 0.2 | (35)[d] |
| $CH_3OH \rightarrow CH_3CH_3$ | 39.5 | 41 | 54.4 ± 0.2 | 42–60[c] |

[a] References 29 and 45. [b] References 7, 8, 49, and 50. [c] References 1, 7, 10, and 11. [d] References 7 and 51.

on the observed $pK_a$'s, the difference is overestimated by ca. 10 kcal/mol owing to the large variation in hydrogen bond strengths noted above.

For the neutral molecules, the accord between theory and experiment is good with an average error of 0.7 kcal/mol. A ladder can be constructed from the $\Delta\Delta G$ values to also show that the order of solubilities from the gas phase is correctly predicted as $CH_3OH > CH_3NH_2 > CH_3CN > CH_3SH > CH_3CH_3$. Moreover, the precision of the computed $\Delta\Delta G$s is confirmed by considering the hystereses for the cycles, $CH_3SH \rightarrow CH_3CH_3 \rightarrow CH_3OH \rightarrow CH_3SH$ and $CH_3S^- \rightarrow CH_3CH_2^- \rightarrow CH_3O^- \rightarrow CH_3S^-$, which amount to only 0.2 and 0.6 kcal/mol, respectively.

Finally, the computed $\Delta\Delta G^{hyd}$'s can be combined with the ab initio results for $\Delta\Delta G_{gas}$ to yield predicted $pK_a$'s relative to $CH_3SH$ and $CH_3OH$. With use of the experimental $pK_a$'s of 10.3 and 15.5 for these reference compounds,[7] the calculated $pK_a$'s in Table VI are obtained from eq 2. For acetonitrile, the predicted $pK_a$ of 28 is a little above the experimental range of roughly 24–27. The apparent discrepancy comes primarily from the overestimate of $\Delta\Delta G_{gas}$ by 6.5 kcal/mol which translates to 4–5 $pK_a$ units. Though the absolute errors in $\Delta G_{gas}$ are small in Table IV, the result for $CH_3SH$ is uniquely below the experimental value. Thus, this is not an issue for the methanol to methylamine conversions, and the predicted $pK_a$ of 33 for methylamine is our best estimate. An experimental result is not directly available in this case; a value of 35 has been proposed by Bell for ammonia[51] and assumed to be appliable to methylamine by Stewart.[7]

The two predictions for the $pK_a$ of ethane in Table VI bracket it at 52 ± 2, which is roughly in the middle of the range of experimental estimates. As mentioned above, the results based on methanethiol and methanol are expected to be on the low and high sides owing to the potential errors in the free energies of hydration of the anions. Some corrections could be made for the differences between the calculated and experimental results for $\Delta\Delta G_{gas}$ in Table VI; however, the uncertainties in the experimental data do not justify this. Overall, the two results for ethane are acceptably consistent and are supported by the reasonable predictions for acetonitrile and methylamine. Though the differences in gas-phase acidities mostly dominate the relative $pK_a$'s in solution for the present acids, the solvent effects are still substantial. For example, the solvent effect for methanol vs ethane makes methanol 20.4 − 6.8 = 13.6 kcal/mol more acidic in water (Table V). Also, the acidity of acetonitrile in water is diminished by 6.5 kcal/mol relative to methanethiol owing to the poorer hydration of $CH_2CN^-$ and the better hydration of $CH_3CN$ relative to $CH_3S^-$ and $CH_3SH$. Similarly, the much poorer hydration of $CH_2CN^-$ than $CH_3O^-$ causes a reversal in the gas-phase and aqueous acidities of acetonitrile and methanol.

**Anion Hydration.** Besides the $pK_a$ estimates, the Monte Carlo simulations afford the opportunity to thoroughly characterize the water structure around the ions. There is much interest in such information, which can also be determined in elegant diffraction work on aqueous solutions, though mostly atomic ions have been studied so far.[52] The focus of the discussions here will be on establishing the number of water molecules that are strongly bound to the ions in the first hydration shell. A key measure of the

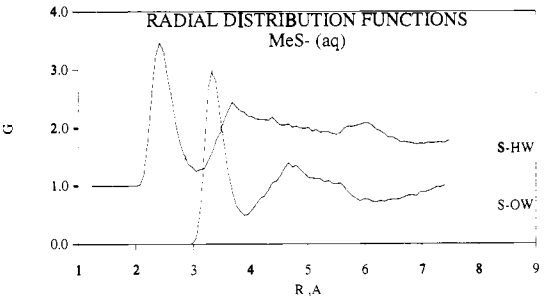


**Figure 6.** Computed S–O and S–H radial distribution functions for $CH_3S^-$ in water. X–H rdf's are offset 1 unit on the ordinate in Figures 6–11.

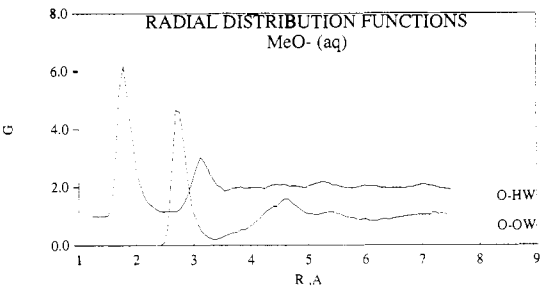


**Figure 7.** Computed O–O and O–H radial distribution functions for $CH_3O^-$ in water.

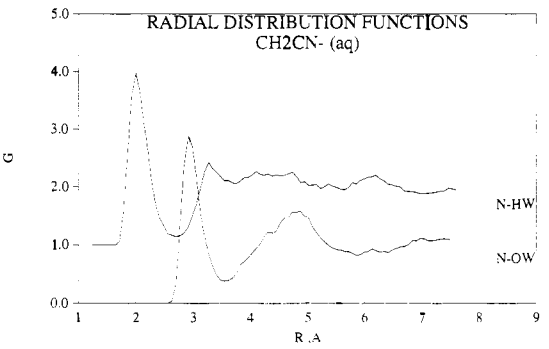


**Figure 8.** Computed N–O and N–H radial distribution functions for $CH_2CN^-$ in water.

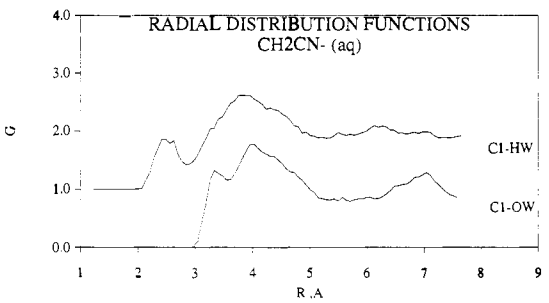


**Figure 9.** Computed $H_2C$–O and $H_2C$–H radial distribution functions for $CH_2CN^-$ in water.

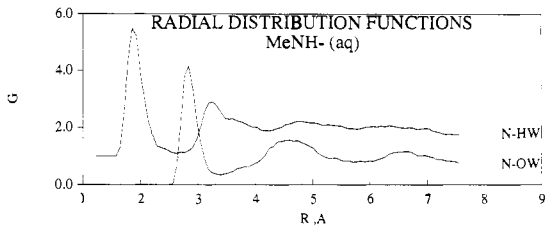


**Figure 10.** Computed N–O and N–H radial distribution functions for $CH_3NH^-$ in water.

(51) Bell, R. P. *The Proton in Chemistry*, 2nd ed.; Cornell University Press: Ithaca, NY, 1973; p 87.

(52) Enderby, J. E.; Cummings, S.; Herdman, G. J.; Neilson, G. W.; Salmon, P. S.; Skipper, N. *J. Phys. Chem.* **1987**, *91*, 5851. Neilson, G. W.; Enderby, J. E. *Annu. Rep. Prog. Chem., Sect. C* **1979**, *76*, 185.

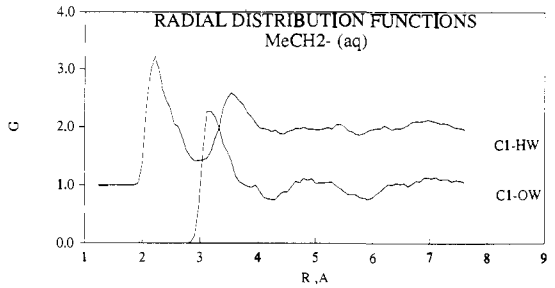


**Figure 11.** Computed $H_2C$–O and $H_2C$–H radial distribution functions for $CH_3CH_2^-$ in water.

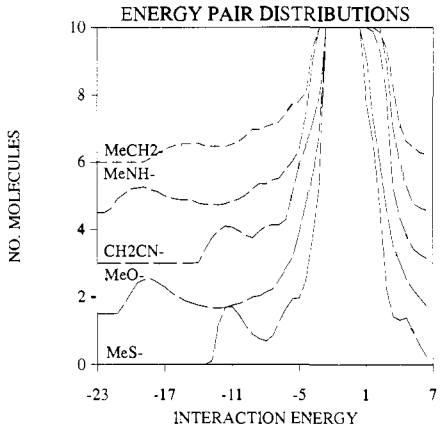


**Figure 12.** Computed distributions of individual anion–water interaction energies (kcal/mol) for the five anions in water. The units for the ordinate are number of water molecules per kcal/mol. Successive plots are offset 1.5 units on the ordinate.

structure is reflected in the radial distribution functions (rdf's), $g_{xy}(r)$, that give the probability of finding an atom of type y at a distance $r$ from an atom of type x in the solution, normalized for the bulk density of x atoms and the radial volume element (eq 7). In the following, x is always an atom of the ion and y

$$g_{xy}(r) = \langle N_y(r, r + dr)\rangle / 4\pi r^2\, dr(N_y/V) \qquad (7)$$

is either the oxygen or a hydrogen of water, $O_w$ or $H_w$. The most informative and structured rdf's from the simulations are recorded in Figures 6–11 and are discussed for the ions individually below. Another important gauge of the energetics of the hydration is provided by the distributions of individual ion–water interaction energies that are displayed in Figure 12.

$CH_3S^-$ is a comparatively straightforward case. The S–H and S–O rdf's in Figure 6 reveal sharp first peaks that reflect the water molecules that are hydrogen-bonded to sulfur. The distinct minima occur at 3.1 and 3.9 Å; integration to these points reveals a coordination number of exactly 6. The assignment of the 6 waters as hydrogen-bonded is then confirmed by the energy pair distribution (Figure 12). The well-resolved band from −12.5 kcal/mol to the minimum at −7.7 kcal/mol is for the most attractive ion–water interactions and also integrates to 6. Thus, there are 6 water molecules hydrogen-bonded to sulfur with an average interaction energy of ca. −11 kcal/mol. These water molecules are also clearly apparent in stereoplots of configurations from the simulations. A random example is provided in the top part of Figure 13. In the plots like this, only the $N$ water molecules with the most attractive interaction energies with the ion are shown, where $N$ is the number of strong hydrogen bonds established from the rdf's and energy pair distributions. The orientation of the water molecules is as expected in Figure 13 for hydrogen bonding to sulfur, though 5 of the water molecules are near enough to the carbon to also enjoy significantly favorable interactions with this atom that has a partial negative charge as well (Table II). Returning to Figure 6, another noteworthy feature is the broad band in the S–O rdf from 4 to 6 Å that is readily assigned to a second hydration shell. In fact, the band undoubtedly includes water

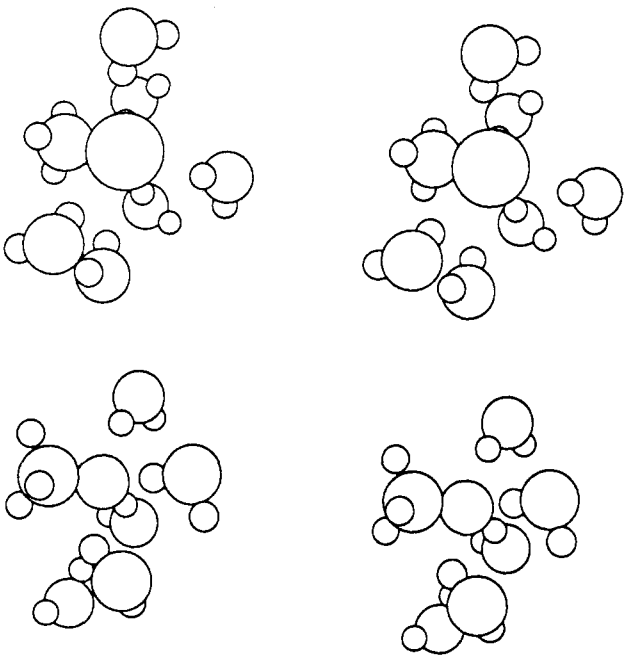

**Figure 13.** Stereoplots of the most bound water molecules around $CH_3S^-$ (top) and $CH_3O^-$ (bottom) from configurations in the Monte Carlo simulations.

molecules in the first layer near the back of the methyl group as well as water molecules that are hydrogen-bonded to the 6 primary waters.

The results for $CH_3O^-$ can also be easily interpreted. The very strong interactions with water are reflected in the sharp first peaks in the O–O and O–H rdf's (Figure 7) and the distinct band in the energy pair distribution from −21 to −12 kcal/mol. Integration to the first minima in each case yields exactly 5 water molecules that form the strong hydrogen bonds to the methoxide oxygen. The tightness of this hydration shell is apparent in the sample stereoplot in the bottom part of Figure 13. The principal reason for the stronger interactions with $CH_3O^-$ than $CH_3S^-$ is the 1.1 Å smaller diameter for the oxygen than for the sulfur atom (Table II), which translates to hydrogen bonds that are ca. 0.6 Å shorter for methoxide (Figures 6 and 7). It may be noted that in earlier Monte Carlo studies, we found analogous hydration numbers of 5 for methoxide ion in methanol[53] and 6 for hydroxide ion in water.[54] The latter result is in agreement with old X-ray data.[55] Recently, Bino has found a $CH_3O^-$-$6H_2O$ unit in an inorganic crystal structure.[56] The small amount of water and high density of ions in the crystal limit the relevance to the present result for a dilute solution. Nevertheless, the number and structure for the coordinating water molecules are similar including the methoxide oxygen–water oxygen distances of 2.7–2.8 Å.

The water structure around $CH_2CN^-$ is a little more complex. The N–O and N–H rdf's are shown in Figure 8, while the Cl–O and Cl–H rdf's are in Figure 9. Comparison of the figures clearly reveals the greater hydrogen bonding at the nitrogen end of the ion. The sharp first peaks in Figure 8 integrate to 4.5. Similarly, the lowest energy band in the energy pair distribution (Figure 12) integrates to 4–4.5 up to the shallow minimum near −9 kcal/mol. Further integration to the inflection point near −6.5 kcal/mol yields an additional 2–2.5 water molecules. These latter solvent molecules appear to be more associated with the carbon terminus; indeed, the small first peaks in the Cl–O and Cl–H rdf's (Figure 9) integrate to 2.4 up to the minima near 2.85 and 3.55 Å, respectively. Thus, the overall picture has 6–7 water molecules hydrogen-bonded to the ion with the majority more attached to

(53) Jorgensen, W. L.; Bigot, B.; Chandrasekhar, J. *J. Am. Chem. Soc.* **1982**, *104*, 4584.
(54) Madura, J. D.; Jorgensen, W. L. *J. Am. Chem. Soc.* **1986**, *108*, 2517.
(55) Brady, G. W. *J. Chem. Phys.* **1958**, *28*, 464.
(56) Bino, A. *J. Am. Chem. Soc.* **1987**, *109*, 275.

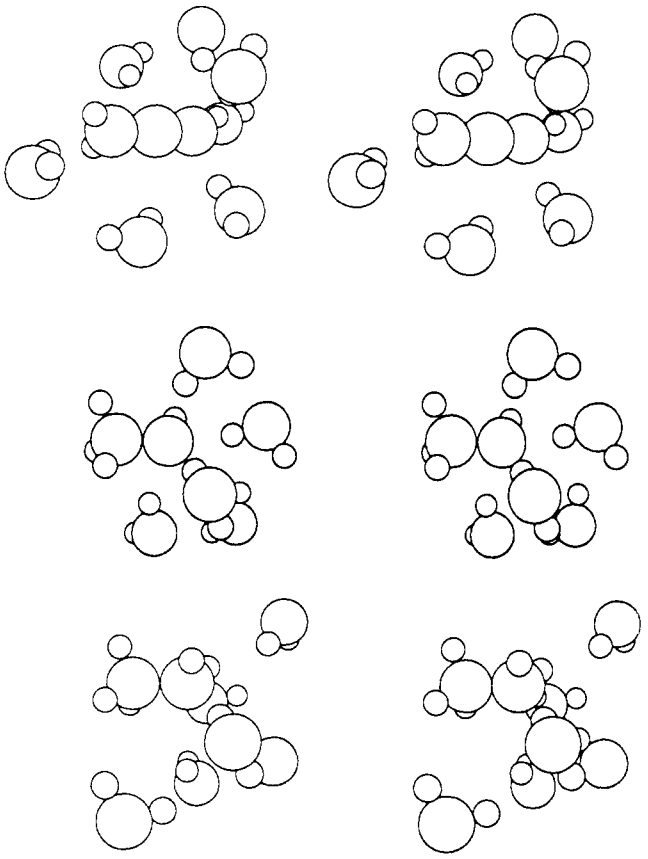

**Figure 14.** Stereoplots of the most bound water molecules around $CH_2CN^-$ (top), $CH_3NH^-$ (middle), and $CH_3CH_2^-$ (bottom) from configurations in the Monte Carlo simulations.

the nitrogen. This is consistent with stereoplots of configurations as in the top of Figure 14.

For $CH_3NH^-$, the N–O and N–H rdf's are shown in Figure 10. The results are similar to those in Figure 7 for methoxide ion with some reduction in structure. Integration of the first peaks in the N–O and N–H rdf's also yields a coordination number of exactly 5. The energy pair distribution in Figure 12 for $CH_3NH^-$ reveals a low-energy band that does not have as sharp a minimum as for $CH_3O^-$ and $CH_3S^-$. However, integration to the actual minimum at −12 kcal/mol yields 4.6 water molecules which grows to 5.0 water molecules up to −10.7 kcal/mol. At least four well-directed hydrogen bonds are apparent with the nitrogen in the sample stereoplot in the middle of Figure 14. It may be noted that these water molecules are shying away from the hydrogen on nitrogen which has a partial positive charge (Table II).

Finally, the Cl–O and Cl–H rdf's for the ethyl anion are shown in Figure 11. Distinct first peaks are evident, though they are broader and lower than for the ions with stronger interactions, $CH_3O^-$ and $CH_3NH^-$. The integral of the Cl–H rdf to the minimum at 2.95 Å encompasses 5.4 water molecules, while the first peak in the Cl–O rdf covers 6.0 water molecules to 3.8 Å. The energy pair distribution for $CH_3CH_2^-$ in Figure 12 is somewhat difficult to analyze since it has no sharp breaks between −19 and −5 kcal/mol. There is a dip at −12 kcal/mol; integration to this point yields 3.0 water molecules. Another 3 water molecules then occur between −12 and −8 kcal/mol. The stereoplot at the bottom of Figure 14 shows that the most bound water molecules congregate near the lone-pair position. There also appear to be 3 water molecules with hydrogens particularly well-directed toward the lone-pair site. In comparison to $CH_3O^-$ where the water molecules surround the anionic oxygen, the hydration of ethyl anion is lopsided with more shielding near the principal anionic site.

## Conclusion

In the present paper, it has been demonstrated that current quantum and statistical mechanical methods can be combined to compute relative $pK_a$'s for organic molecules in water. Good accord with experiment is found for the computed gas-phase acidities and relative free energies of hydration for the neutral molecules. The computed $pK_a$'s seem reasonable, and an estimate in the low fifties has been provided for the controversial $pK_a$ of ethane. The greatest point of concern in the calculations is the lack of explicit treatment of polarization effects in the potential functions and solution simulations. Along these lines, it is interesting to note some recent results for the hydration of chloride ion that used the same procedures for developing the anion–water potential functions and for the Monte Carlo simulations as in the present work.[16] The absolute free energy of hydration was computed by perturbing $Cl^-$ to nothing in TIP4P water. The result of −79 ± 2 kcal/mol, which included a simple Born correction for the interactions neglected beyond the 8.5 Å cutoff, is in exact accord with experimental estimates. This suggests along with other results[32,47] that polarization effects are included in an average sense in the potential functions. However, the errors unquestionably mount as the ion–water interactions become stronger.[47] To minimize this influence, it is advisable to compare compounds that have similar individual anion–water interaction energies, as has been done here.

The Monte Carlo simulations also provided detailed information on the hydration of the anions. The numbers of uniquely strong anion–water hydrogen bonds were found to be five for $CH_3O^-$ and $CH_3NH^-$ and six for $CH_3S^-$. The $CH_2CN^-$ ion has 6–7 water molecules in the first hydration layer with 4–5 well bound near the nitrogen, while there are 3 water molecules that hydrogen bond to the anionic carbon of $CH_3CH_2^-$ with another 3 water molecules in close proximity. These predictions stand for future tests by experimental methods. Overall, the potential for quantitatively meaningful theoretical studies of organic chemistry in solution has been further illustrated.[57,58]

**Acknowledgment.** Gratitude is expressed to the National Science Foundation and National Institutes of Health for support of this research. Computational assistance from Dr. Jiali Gao is also gratefully acknowledged.

**Registry No.** $CH_3SH$, 74-93-1; $CH_3OH$, 67-56-1; $CH_3CN$, 75-05-8; $CH_3NH_2$, 74-89-5; $CH_3CH_3$, 74-84-0.

**Supplementary Material Available:** The geometries in Z-matrix format, total energies computed for the neutral molecules and anions, and summary figures on the results for the 22 anion–water complexes (12 pages). Ordering information is given on any current masthead page.

(57) Jorgensen, W. L. *Adv. Chem. Phys.* **1988**, *70 (Part II)*, 469.
(58) Jorgensen, W. L. *Acc. Chem. Res.*, in press.